High-temperature manganese diffusion into KDB-3 silicon: formation of Mn_5Si_3 and B_6Si phases, morphology and electrophysical properties

© N.F. Zikrillaev[1], S.O. Saidov[2], N.Yu. Sharibaev[3], G.Kh. Mavlonov[1], I.A. Abduganiev[1], E.S. Nazarov[2], I.O. Kosimov[4], A.K. Ergashov[3]

[1] Tashkent State Technical University named after Islam Karimov,
100095 Tashkent, Uzbekistan
[2] Bukhara State University,
200118 Bukhara, Uzbekistan
[3] Namangan State Institute of Engineering and Technology,
160103 Namangan, Uzbekistan
[4] A. Sadykov Institute of Bioorganic Chemistry,
100125 Tashkent, Uzbekistan

E-mail: safo.saidov.64@mail.ru

Received July 25, 2025
Revised November 27, 2025
Accepted December 28, 2025

The formation of structural, phase and electrophysical properties of KDB-3 silicon after high-temperature manganese diffusion at 1100 °C in a sealed ampoule is investigated. X-ray phase analysis shows the formation of a surface two-phase layer containing intermetallic Mn_5Si_3 and borosilicide B_6Si, with a high fraction of amorphous component. Scanning electron microscopy reveals a pronounced multi-scale relief comprising macro-, micro- and nanostructured elements that reflect heterogeneous material redistribution during diffusion. Electrophysical measurements demonstrate a significant increase in resistivity, reduction of carrier mobility and decrease in carrier concentration, which are attributed to the combined effect of the amorphous matrix and distributed silicide inclusions. The results establish clear links between phase composition, morphology and charge transport in Si:Mn and clarify mechanisms governing the functional properties of modified KDB-3 silicon.

Keywords: KDB-3 silicon, manganese diffusion, phase composition, Mn_5Si_3, B_6Si, surface morphology, X-ray phase analysis, electrophysical properties.

DOI: 10.61011/SC.2025.10.62868.8429

1. Introduction

High-temperature diffusion of transition metals into silicon is an effective method for controlled modification of near-surface layers and for changing their structural and electrophysical properties. The behavior of 3*d* impurities in silicon is determined by their solubility at elevated temperatures, by interaction with the dopant components of the substrate, and by the formation of stable silicide compounds. These processes are controlled by the processing temperature, the annealing time, and the cooling regime, which determine the phase composition and the degree of structural reconfiguration of the material.

The Si−Mn systems are of interest due to the possibility of forming the intermetallic phase Mn_5Si_3, which has a stable crystalline structure and specific electronic properties. Modern studies confirm the reproducibility of Mn_5Si_3 formation on silicon substrates at elevated temperatures. Mn has limited solubility in bulk Si; however, at elevated temperatures, at high T surface segregation occurs, which promotes the formation of Mn_5Si_3 and makes this phase's morphology sensitive to the sample preparation conditions [2–4]. This phase plays a key role in the structural organization of the surface layer in Si−Mn systems and is currently the subject of active research.

For a reliable interpretation of structural transformations, a comprehensive methodological approach is used: X-ray diffraction (XRD) provides identification of the formed compounds; scanning electron microscopy/energy-dispersive X-ray spectroscopy (SEM/EDS) makes it possible to investigate the surface morphology and nanostructure features; the use of software for processing diffraction data (search-match, qualitative analysis, and RIR (Reference Intensity Ratio) quantification) improves the reliability of phase identification.

In this work, silicon KDB-3 subjected to high-temperature manganese diffusion under 1100 °C was investigated. The aim of this study was to establish the relationship between the phase composition of the near-surface layer (Mn_5Si_3, B_6Si), the surface morphological features, and the electrophysical characteristics of the modified layer. To achieve this aim, X-ray diffraction analysis, microstructural studies (SEM), electrophysical measurements, and a complete set of primary experimental data were prepared to ensure transparency and reproducibility of the results [6].

2. Methods and experimental results

2.1. Samples and manganese diffusion procedure

As the starting material, boron-doped single-crystal silicon wafers (as-received) of KDB-3 grade with (100) orientation and resistivity $\rho \approx 3\,\Omega\cdot$cm were used. Prior to thermal

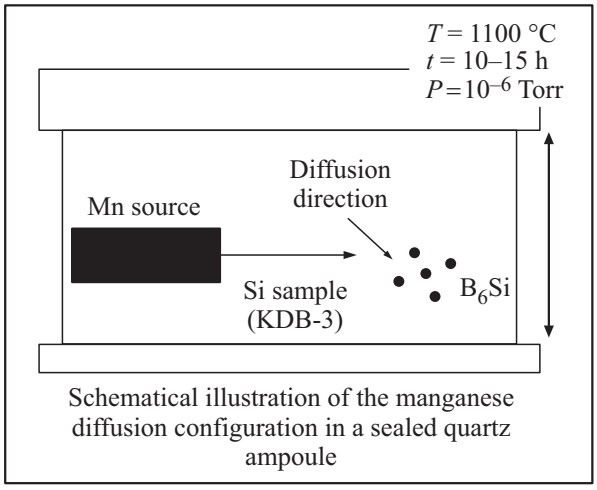

Figure 1. Schematic representation of the Mn diffusion process in KDB-3 silicon at 1100 °C.

treatment, standard chemical cleaning using the RCA cleaning procedure [7] was performed, and the near-surface silicon layer of thickness $\sim 100\,\mu$m was removed. Such preparation makes it possible to exclude the influence of near-surface regions with an increased impurity concentration and ensures the reproducibility of the subsequent high-temperature diffusion [5].

Manganese diffusion was carried out in sealed quartz ampoules. Silicon samples were placed in the ampoule together with metallic Mn; the system was then evacuated to a residual pressure of $\sim 10^{-6}$ mm Hg and sealed. The main parameters and a schematic representation of the Mn diffusion process in silicon KDB-3 are given in Table 1 and Figure 1, respectively. Heating was performed in a tube diffusion furnace at a rate of 10–15 °C/min up to a temperature of 1100 °C, at which the phase Mn_5Si_3 forms stably in the Si–Mn system and boron in the initial KDB-3 is thermally activated, which leads to the formation of B_6Si. The B_6Si phase forms solely due to redistribution of the as-received boron in the KDB-3 substrate at 1100 °C; no additional boron doping was performed. Holding at the maximum temperature for 10–15 h ensured a quasi-steady state and the formation of stable silicides in the Si–Mn–B system [1,3]. Upon completion of the annealing, the ampoules were removed from the furnace and rapidly cooled to room temperature. This cooling regime suppresses further Mn redistribution and limits the growth of large silicide inclusions. It has previously been shown that high-temperature processes in a sealed volume at temperatures of ~ 1100 °C lead to the formation, in the near-surface region of silicon, of the intermetallic phase Mn_5Si_3 and, in the presence of boron, borosilicide compounds B_6Si [2–6]. As shown above, Mn exhibits low solubility in bulk Si; at elevated temperatures it preferentially accumulates in the near-surface region, where its enrichment triggers the nucleation of the silicide phase Mn_5Si_3. Both experimental and theoretical studies of Mn adsorption and diffusion on Si corroborate Mn's propensity to form silicide clusters and layers at elevated temperatures [8,9]. The obtained samples were subjected to a comprehensive characterization of structural, morphological, and elemental features using XRD and SEM/EDS [4]. This methodological set provides a coherent structure-morphology analysis and enables assessment of how high-temperature diffusion conditions affect the formation of surface phases and microstructure.

Table 1. Key parameters of Mn diffusion

Parameters	Value/description
Substrate type	Single-crystal Si KDB-3, (100), *p*-type, $\rho \approx 3\,\Omega\cdot$cm
Mn incorporation method	Solid-state diffusion from a metallic source in a sealed ampoule
Diffusion temperature	1100 °C
Annealing time	10–15 h
Vacuum (residual pressure)	$\sim 10^{-6}$ mm Hg
Heating rate	10–15 °C/min
Cooling regime	Rapid cooling

High-temperature Mn diffusion in a sealed volume at 1100 °C results in the formation of a stable two-component near-surface layer Mn_5Si_3–B_6Si, which governs the subsequent morphological and electrophysical characteristics of the modified KDB-3 silicon. The described high-temperature diffusion methodology establishes the initial conditions for the phase composition and microstructure of the near-surface layer. In the following section, the XRD results are presented, enabling quantitative confirmation of the formation of the Mn_5Si_3 and B_6Si phases and correlation of their emergence with the processing conditions.

2.2. X-ray diffraction (XRD) phase analysis

X-ray diffraction (XRD) measurements of the modified KDB-3 sample were performed using the θ–2θ scanning mode on a Shimadzu diffractometer (Cu$K\alpha$, $\lambda = 1.5406$ Å) in the $2\theta = 5$–$70°$ range, with a step of 0.050° and a scan rate of 2 °/min. Primary processing of the XRD data was then carried out.

2.2.1. Overall diffraction pattern

In the experimental diffraction pattern (Figure 2), the following features are observed: a set of intense reflections from the crystalline silicon substrate, a series of broad low-intensity maxima of Mn silicides (Mn–Si), and a pronounced amorphous background in the low-angle region. The appearance of an amorphous component and the broadening of reflections are associated with high-temperature manganese diffusion at 1100 °C, accompanied by partial disruption of the initial crystallinity of the upper Si layer [1,2].

Table 2. Diffraction peak parameters of the KDB-3 sample

No. of peak	2θ, deg.	d, Å	I/I_o, %	FWHM, deg.	Intensity	Integrated intensity
1	9.031	9.7883	132.66	1.3000	1855.74	13715
2	13.432	6.5853	54.68	1.4000	823.70	–
3	37.582	2.3918	381.02	0.2000	819.98	12855
4	43.372	2.0849	68.56	0.5000	368.85	4121
5	43.807	2.0649	1000.00	0.2500	5951	30717
6	47.418	1.9157	92.54	0.2000	199.16	3250
7	48.012	1.8933	71.31	0.2000	153.47	2638
8	50.485	1.8061	53.36	0.2500	143.54	2137
9	56.195	1.6353	133.51	0.3000	430.97	5332
10	64.168	1.4500	133.51	0.2500	2402	12553

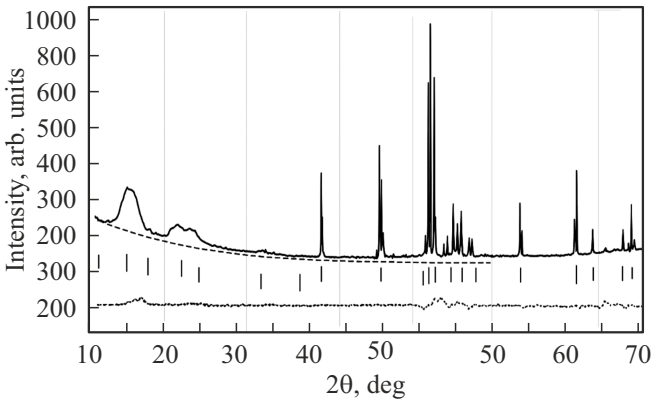

Figure 2. X-ray diffraction profile of the KDB-3 sample: experimental diffractogram (solid line), calculated reflection positions of the B_6Si and Mn_5Si_3 phases (short vertical ticks), fitted background (dashed line), and the „experiment–RIR model" difference curve (dotted line).

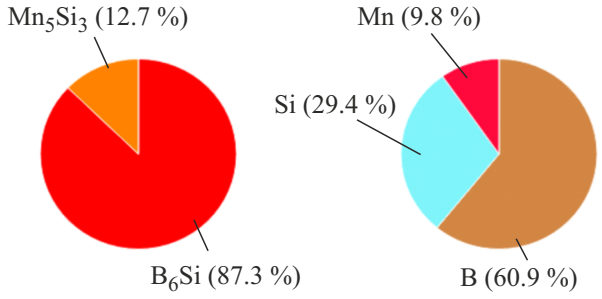

Figure 3. Phase (left) and elemental (right) compositions of the diffusion layer of the KDB-3 sample.

Phase identification and quantitative analysis revealed the presence of two main phases: Phase 1: B_6Si — 87.3 % Phase 2: Mn_5Si_3 — 12.7 %. The phase composition diagrams are presented in Figure 3. The Mn_5Si_3/B_6Si ratio is consistent with current data on the stability of silicides in the Mn–Si system and with trends in Mn segregation near the silicon surface at temperatures ~ 1100 °C [10]. The presence of weak-diffraction maxima of Mn–Si compounds is corroborated by results of other studies on structuring Mn_5Si_3 thin-film and high-temperature-treated systems [11].

2.2.2. Degree of crystallinity and amorphous fraction

The degree of crystallinity is as follows: DOC = 23.59 %, amorphous fraction ≈ 76.41 %. A high amorphous contribution is an expected outcome of Mn diffusion in Si followed by rapid cooling, which stabilizes a disordered structure [12]. Similar DOC levels are typical of strongly modified silicon layers after high-temperature cycles, as also observed in other Si systems doped with transition-metal impurities.

2.2.3. Diffraction peak parameters (XRD)

The positions and parameters of the main diffraction peaks are listed in Table 2. The most intense diffraction reflections are as follows: The reflections at $2\theta = 43.807$, 37.582, 64.168° correspond to the characteristic peaks of Mn_5Si_3 and B_6Si, respectively, which is consistent with literature data on the symmetry and interplanar spacings of these compounds [11].

The relatively low intensity of the Si reflections (regions 47.4 and 56.2°) confirms partial degradation of the crystalline Si substrate layer after Mn diffusion [2].

2.2.4. Local analysis of the range 35–44°

A diffractogram fragment in the 35–44° range (Figure 4) contains five distinct maxima, two of which at 37.582 and 43.807° are assigned to Mn_5Si_3 (Table 3). The remaining peaks have shapes and widths typical of fine-grained silicides, indicating an inhomogeneous distribution of Mn-containing phases.

The absence of intense Si reflections in this range confirms amorphization of the surface layer.

Table 3. Crystallite size estimation of Mn_5Si_3 using the Scherrer method

2θ, deg.	FWH_{meas}, deg.	β_{inst}, deg.	β_{corr}, deg.	D, nm
37.5823	0.23390	0.22770	0.0326	≈ 30
43.8074	0.23370	0.22770	0.0317	≈ 28

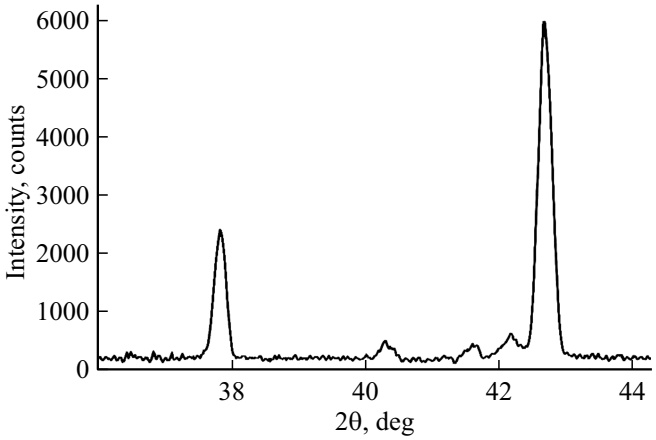

Figure 4. Fragment of the diffraction pattern ($35-44^\circ$, 2θ).

2.2.5. Crystallite size estimation of Mn_5Si_3 using the Scherrer method

The experimental FWHM values of the Mn_5Si_3 reflections are close to the diffractometer's instrumental resolution. For the $\beta_{corr} < 0.04^\circ$ reflection, the Scherrer equation loses sensitivity, and the derived crystallite sizes become indeterminate (instrument-limited regime). Such behavior is characteristic of coarse-grained Mn_5Si_3 inclusions ($\gg 100$ nm) formed during high-temperature diffusion and the slow approach to the equilibrium phase composition [3,4]. The instrumental contribution to peak broadening was assumed to be $\beta_{inst} = 0.2277^\circ$, which corresponds to the narrowest silicon reflection at $2\theta = 47.418^\circ$. The correction for experimental peak broadening was performed using the expression:

$$\beta_{corr} = \sqrt{\beta^2_{meas}} - \beta^2_{inst}.$$

The crystallite size was calculated using the Scherrer equation:

$$D = \frac{K\lambda}{\beta_{corr}\cos\theta},\ K = 0.9,\ \lambda = 1.5406\,\text{Å},\ \theta = \frac{1}{2}2\theta.$$

The diffusion-layer structure revealed by XRD is characterized by a stable combination of phases $Mn_5Si_3-B_6Si$, a high degree of amorphization, and large silicide inclusions. XRD analysis demonstrates that high-temperature Mn diffusion leads to the formation of a phase-inhomogeneous, amorphous-crystalline structure, in which large Mn_5Si_3 inclusions are „frozen" into an amorphous B_6Si-Si matrix, which determines the key morphological and electrophysical properties of the modified silicon KDB-3. The obtained structural data provide the basis for interpreting the morphological features of the surface layer and their impact on charge transport, which is discussed in the following section.

2.3. Surface morphology of the KDB-3 sample

The surface morphology of the modified silicon layer of KDB-3 was examined by scanning electron microscopy using a JEOL JSM-IT210 instrument at an accelerating voltage of 10 kV. To ensure stable charge dissipation, carbon coating was applied using a JEOL JEC-3000FC sputter coater. The analysis was performed on a series of images acquired at magnifications from $\times 100$ to $\times 2700$, which makes it possible to trace the relief structure over a broad range of length scales (Figure 5, *a–e*).

At low magnifications $\times 100-270$ (Figure 5, *a, b*), the surface exhibits pronounced large-scale nonuniformity. Disordered macro-regions with a characteristic size of $\sim 50-200\,\mu$m are observed, separated by grooves and depressions, which reflects substantial restructuring of the surface layer under high-temperature treatment. The mosaic distribution of regions with different density is associated with nonuniform Mn incorporation and local Mn segregation during diffusion. At higher magnifications $\times 550-1000$ (Figure 5, *c, d*), a developed microstructure becomes apparent, represented by aggregates of irregular shape with sizes of $3-10\,\mu$m. Their boundaries are rough and partially fragmented, indicating competing processes of growth, degradation, and redistribution of the material. The inter-aggregate regions contain submicron particles with sizes of 200–500 nm, forming a transition layer between large and fine morphological features. The maximum magnification $\times 2700$ (Figure 5, *e*) reveals a complex nanorelief. Against the background of a weakly ordered matrix, elongated platelet-like elements with a length of $0.5-2.5\,\mu$m and a width of up to several hundred nanometers are observed, as well as dense clusters of nanograins with sizes of 80–300 nm. The simultaneous presence of platelet-like and granular morphological components indicates a multistage structural reorganization of the near-surface layer during high-temperature Mn diffusion. Thus, the surface of the diffusion-modified KDB-3 sample is characterized by a hierarchically organized multiscale relief, including large disordered regions (tens to hundreds of micrometers), micrometer-sized irregular fragments ($3-10\,\mu$m), a submicron granular component (200–500 nm), and nanostructured platelet-like and granular elements (80–300 nm). Such a multilevel morphology is consistent with the XRD structural results (Section 2.2), reflecting the combined effect of phases $Mn_5Si_3-B_6Si$ and a high degree of amorphization on the formation of the surface relief. The obtained data indicate a complex thermally induced restructuring of the material during Mn diffusion, which ultimately determines the electrophysical properties of the modified silicon.

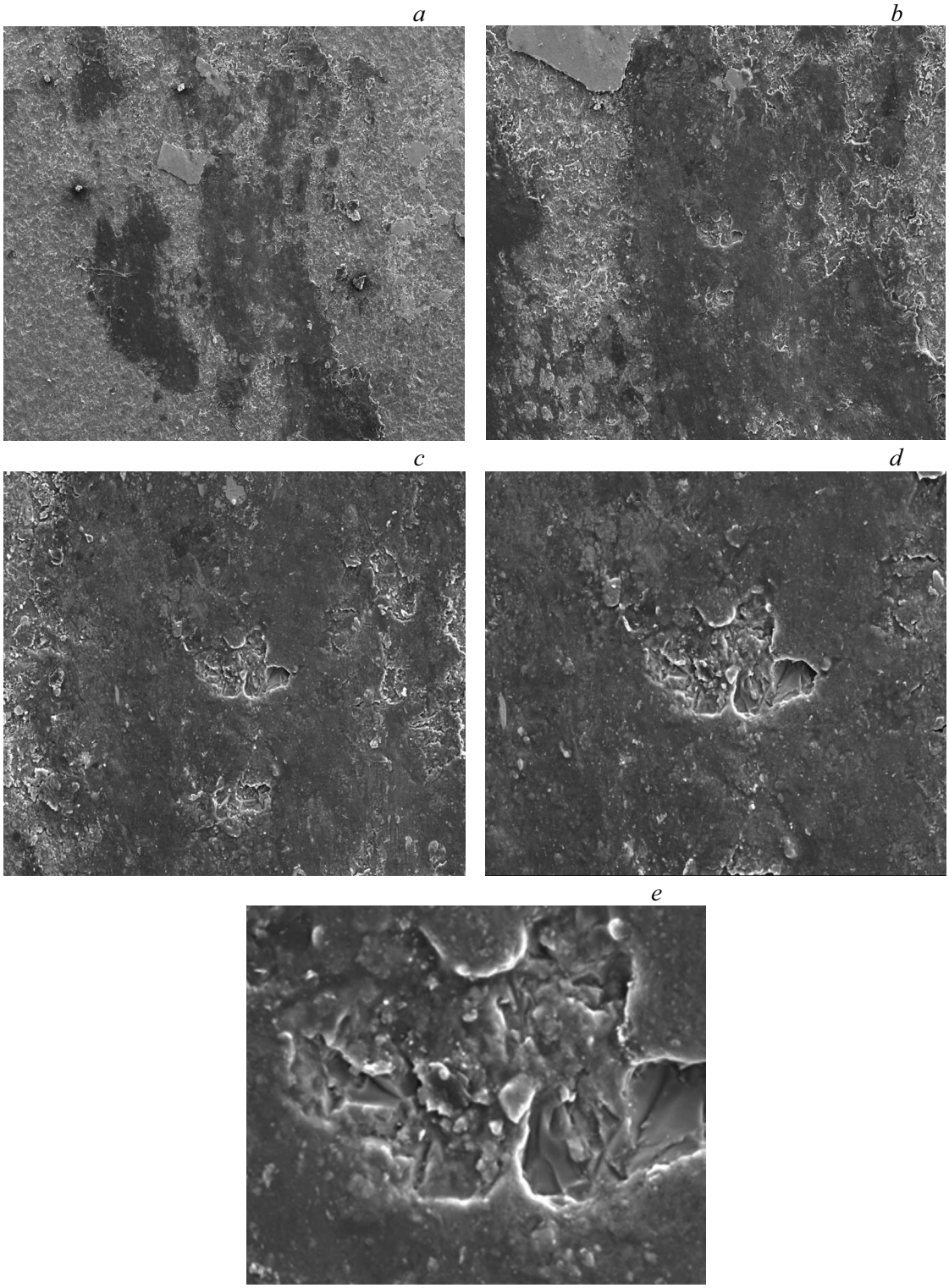

Figure 5. SEM images of the surface of the KDB-3 sample after high-temperature Mn diffusion.

The hierarchical morphology revealed by SEM is consistent with the phase-structural features established by XRD analysis. This consistent picture provides the prerequisites for analyzing the electrophysical properties of the diffusion-modified silicon layer of KDB-3.

3. Electrophysical characteristics of the Si:Mn system

The electrophysical properties of the modified silicon KDB-3 are determined by a set of structural factors formed

during high-temperature Mn diffusion. X-ray phase analysis revealed the formation of a two-phase silicide structure $Mn_5Si_3-B_6Si$ at a high degree of near-surface-layer amorphization ($\approx 76\,\%$), whereas the morphological studies showed the presence of coarse silicide inclusions and a well-developed nanorelief component. Such a combination of phases and morphological features forms an inhomogeneous conducting medium that exerts a decisive influence on the character of charge transport [13].

Longitudinal-geometry measurements under an applied magnetic field of $B = 0.14\,\mathrm{T}$ yielded Hall voltages of $U_{\delta 1} = 896\,\mathrm{mV}$ and $U_{\delta 2} = 953\,\mathrm{mV}$. The mean value of $U_{\delta,\,\mathrm{ave}} = 924.5\,\mathrm{mV}$ was used to calculate the transport parameters at an average current of $I_{\mathrm{ave}} = 0.0405\,\mathrm{mA}$. Based on the sample geometry (thickness $W = 0.8\,\mathrm{mm}$ and width $d = 3.5\,\mathrm{mm}$), the longitudinal resistance was determined to be $R_{xx} \approx 1.4 \cdot 10^5\,\mathrm{Ohm}$, and the resistivity of the near-surface layer was $\rho \approx 2.3 \cdot 10^3\,\mathrm{Ohm \cdot cm}$. The charge-carrier concentration $n \approx 4.5 \cdot 10^{13}\,\mathrm{cm^{-3}}$ and the mobility $\mu \approx 60\,\mathrm{cm^2/(V \cdot s)}$ differ markedly from the initial parameters of KDB-3 silicon, which is associated with Mn redistribution and the formation of an amorphous matrix and silicide clusters. The conducting regions Mn_5Si_3 form local channels of enhanced conductivity within the more weakly conducting matrix B_6Si-Si. Their spatially fragmented distribution forms a network of interphase boundaries and localized potential barriers, which results in spatially inhomogeneous charge transport and promotes the development of interphase polarization [14]. The presence of nanograined and platelet-like elements further increases the effective area of interphase interfaces, enhancing the role of traps and localized states. The increasing fraction of the amorphous component promotes a reduction in carrier mobility and an increase in resistivity. The obtained structural features of the Mn_5Si_3 phase are consistent with modern data on nonstoichiometry and secondary phase relations in Mn–Si systems [15].

To estimate the Mn diffusion parameters, a standard expression $D = D_0 \exp(-E_a/kT)$ was used, where the temperature $T = 1100\,^\circ\mathrm{C}$ corresponds to the diffusion-treatment conditions. The estimated diffusion length $X = 2\sqrt{(Dt)}$ is consistent with the formation of a silicide layer several micrometers thick, as inferred from the structural data. Taken together, the electrophysical measurements show that charge transport in the Si:Mn system is determined by competition between the conducting regions Mn_5Si_3 and the highly ordered B_6Si-Si matrix. This structural-phase architecture gives rise to complex, spatially inhomogeneous charge transport that is directly linked to the morphological features of the near-surface layer identified in Sections 2.2 and 2.3. The obtained electrophysical parameters, considered together with the phase and morphological analyses, confirm the key role of high-temperature Mn diffusion in the formation of a multilayer structure comprising the $Mn_5Si_3-B_6Si-Si$ phases, which governs the functional properties of the modified KDB-3 silicon. These results provide the basis for the overall conclusions of the study.

4. Conclusion

High-temperature Mn diffusion in KDB-3 silicon leads to the formation of a complex multicomponent near-surface structure comprising the Mn_5Si_3 and B_6Si phases, together with a significant amorphous contribution. X-ray diffraction analysis indicates that this configuration is accompanied by a reduced degree of crystallinity and the appearance of broadened diffraction maxima from the silicide phases. Morphological studies confirm the presence of a multiscale surface relief comprising macro-, micro-, and nanostructured features associated with nonuniform silicide formation and amorphization processes.

Electrophysical measurements revealed a pronounced increase in resistivity and a decrease in carrier mobility, which is attributed to the formation of a spatially inhomogeneous conducting medium consisting of local conducting regions embedded in a less conductive Si matrix. The spatial distribution of silicide inclusions and the developed network of interphase boundaries govern the inhomogeneous nature of charge transport and enhance the contribution of localized states.

Taken together, the structural, morphological, and transport data demonstrate the coupled impact of phase composition, amorphization, and the spatial distribution of silicide inclusions on the electrophysical properties of the Si:Mn system. These results refine the mechanism of Mn-driven silicon modification during high-temperature diffusion and provide a basis for developing functional materials based on transition-metal silicides.

Conflict of interest

The authors declare that they have no conflict of interest.

References

[1] M.K. Bakhadyrkhanov, Kh.M. Iliev, M.O. Tursunov, S.B. Isamov, S.V. Koveshnikov, M.K. Madjitov. Inorg. Mater., **57**, 655 (2021). DOI: 10.1134/S0020168521070027

[2] N.F. Zikrillayev, M.M. Shoabdurahimova, T. Kamilov, A.Z. Khusanov, K.K. Kurbonaliev, N. Norkulov, E.B. Saitov. Phys. Sci. Technol., **9**, 89 (2022). DOI: 10.1109/PST55267.2022.00020

[3] H. Li, D. Niu, Z. Zhang, F. Yang, H. Wang, W. Cheng. Materials, **16**, 3540 (2023). DOI: 10.3390/ma16103540

[4] I. Kounta, H. Reichlová, D. Kriegner, X. Marti, T. Jungwirth, J. Kuneš. Phys. Rev. Mater., **7**, 024416 (2023). DOI: 10.1103/PhysRevMaterials.7.024416

[5] D.I. Rogilo, S.V. Sitnikov, E.E. Rodyakina, and A.A. Shklyaev. Kristallografiya, **66** (528), 2021 (2021). (in Russian). DOI: 10.31857/S0023476121060101

[6] J. Rial, A. Bhowmik, I. Kezsmarki, D. Kriegner, H. Reichlová, X. Marti. Phys. Rev. B, **110**, L220411 (2024). DOI: 10.1103/PhysRevB.10.L220411

[7] Kh.F. Zikrillaev, K.S. Alopov, G.Kh. Mavlonov, and F.Kh. Karimov. FTP, **56**, 528 (2022). (in Russian). DOI: 10.21883/FTP.2022.06.52664.9760
[8] W. Kern. J. Electrochem. Soc., **137** (6), 1887 (1990). DOI: 10.1149/1.2086825
[9] M. Hortamani, V.G. Ruiz, A. Qadeer, P. Kratzer, M. Scheffler. Phys. Rev. B, **74**, 205305 (2006). DOI: 10.1103/PhysRevB.74.205305
[10] N.S. Chauhan, S.G. Sara, A. Bhattacharya, T. Mori, Y. Miyazaki. Adv. Funct. Mater., **34**, 2313948 (2024). DOI: 10.1002/adfm.202313948
[11] S.-H. Kim, J.-H. Park, J.-K. Lee. Appl. Surf. Sci., **622**, 156821 (2023). https://doi.org/10.1016/j.apsusc.2023.156821
[12] H. Reichlová, R.L. Seeger, R. González-Hernández, I. Kounta, R. Schlitz, D. Kriegner, P. Ritzinger, M. Lammel, M. Leiviskä, A.B. Hellenes, K. Olejník, V. Petříçek, P. Doležal, L. Horák, E. Schmoranzerová, A. Badura, S. Bertaina, A. Thomas, V. Baltz, L. Michez, J. Sinova, S.T.B. Goennenwein, T. Jungwirth, L. Šmejkal. Nature Commun., **15**, 4961 (2024). https://doi.org/10.1038/s41467-024-48493-w
[13] D. Senk, G. Borchardt. Microchim. Acta, **80**, 477 (1983). https://doi.org/10.1007/BF01200866
[14] R. Ume, H. Gong, V. Tokranov, M. Yakimov, K. Brew, G. Cohen, C. Lavoie, S. Schujman, J. Liu, A.I. Frenkel, K. Beckmann, N. Cady, S. Oktyabrsky. J. Appl. Phys., **132** (3), 035103 (2022). DOI: 10.1063/5.0096022
[15] M. Idrees, M.W. Khurami, B. Amin, Y. Chen, X. Yan. Mater. Sci. Semicond. Process., **163**, 107593 (2023). DOI: 10.1016/j.mssp.2023.107593

Translated by A.Akhtyamov